Human Ribonuclease with a Pendant Poly(Ethylene Glycol) Inhibits Tumor Growth in Mice[1]

Thomas J. Rutkoski*, John A. Kink†, Laura E. Strong† and Ronald T. Raines*,‡

*Department of Biochemistry, University of Wisconsin-Madison, Madison, WI; †Quintessence Biosciences, Inc, Madison, WI; ‡Department of Chemistry, University of Wisconsin-Madison, Madison, WI

Abstract

Human pancreatic ribonuclease (RNase 1) is a small secretory protein that catalyzes the cleavage of RNA. This highly cationic enzyme can enter human cells spontaneously but is removed rapidly from circulation by glomerular filtration. Here, this shortcoming is addressed by attaching a poly(ethylene glycol) (PEG) moiety to RNase 1. The pendant has no effect on ribonucleolytic activity but does increase persistence in circulation. The RNase 1–PEG conjugates inhibit the growth of tumors in a xenograft mouse model of human lung cancer. Both retention in circulation and tumor growth inhibition correlate with the size of the pendant PEG. A weekly dose of the 60-kDa conjugate at 1 μmol/kg inhibited nearly all tumor growth without affecting body weight. Its molecular efficacy is ∼5000-fold greater than that of erlotinib, which is a small molecule in clinical use for the treatment of lung cancer. These data demonstrate that the addition of a PEG moiety can enhance the *in vivo* efficacy of human proteins that act within cells and highlight a simple means of converting an endogenous human enzyme into a cytotoxin with potential clinical utility.

Translational Oncology (2013) **6**, 392–397

Introduction

An impediment to the development of proteins as chemotherapeutic agents is the dearth of human proteins that can act as cytotoxins. One exception is human pancreatic ribonuclease (RNase 1) [1–3]. Like RNase A (which is its storied bovine homolog [4–6]), RNase 1 catalyzes the cleavage of single-stranded RNA after pyrimidine residues. As a highly cationic protein, RNase 1 can enter the cytosol of human cells spontaneously and there manifest cytotoxic ribonucleolytic activity [7–9]. As a small protein, RNase 1 is cleared rapidly from circulation through glomerular filtration [10,11]. A simple variant of RNase 1 is now in a phase 1 clinical trial as a cancer chemotherapeutic agent [12], and we reasoned that the installation of a poly(ethylene glycol) (PEG) moiety could enhance the utility of RNase 1 by increasing its persistence in circulation [13–15].

RNase 1 has no free cysteine residues. Hence, site-directed mutagenesis can be used to install a unique sulfhydryl group that could be linked to a PEG moiety. Because RNase 1 has 128 residues, the ensuing PEGylated enzyme would be >99% identical in amino acid sequence to an endogenous human protein. Previously, various aspects of this semisynthetic strategy have shown promise with other ribonucleases and nucleases from plants [16–18] and animals [19–22]. Deleterious immunologic responses could, however, compromise the utility of these foreign proteins in the clinic. Accordingly, we sought to validate the strategy with a human enzyme.

Herein, we report on the preclinical attributes of site-specific PEG conjugates to RNase 1. Despite their low cytotoxic activity *in vitro*, we find that these conjugates are highly efficacious in inhibiting the growth of tumors in xenograft mouse models. This work opens a new frontier in the development of anticancer drugs based on human proteins.

Materials and Methods

Materials

Escherichia coli BL21(DE3) cells and pET22b(+) plasmid were from Novagen (Madison, WI). Cell lines K-562 (human chronic myelogenous leukemia) and A549 (human alveolar adenocarcinoma) were from the American Type Culture Collection (Manassas, VA). Homozygous male athymic (*nu/nu*) mice were from Harlan Laboratories (Indianapolis, IN). Cell culture medium and supplements [including Dulbecco's phosphate-buffered saline (PBS)] were from Invitrogen (Carlsbad, CA).

Erlotinib hydrochloride (Tarceva) was from Genentech (South San Francisco, CA). [*Methyl*-^{3}H]thymidine (6.7 Ci/mmol) was from PerkinElmer (Boston, MA). RNase 1 substrate 6-FAM-dArUdAdA-6-TAMRA was from Integrated DNA Technologies (Coralville, IA). Both linear mPEG-maleimide (5 and 20 kDa; **1** and **2**) and branched mPEG$_2$-maleimide (60 kDa; **3**; Figure 1*A*) were from Nektar Therapeutics (Huntsville, AL). Chromatography columns and resins were from GE Healthcare (Uppsala, Sweden). Gel filtration standards, sodium dodecyl sulfate–polyacrylamide gel electrophoresis molecular weight standards, and precast gels for poly(acrylamide) electrophoresis were from BioRad (Hercules, CA). The BCA protein assay kit was from Pierce (Rockford, IL). Black nontreated 96-well plates for pharmaco-

kinetic assays were from NUNC (Rochester, NY). All other chemicals used were of commercial reagent grade or better and were used without further purification.

Analytical Instruments

The mass of purified proteins was confirmed by matrix-assisted laser desorption ionization–time of flight (MALDI-TOF) mass spectrometry using a Voyager-DE-PRO Biospectrometry Workstation from Applied Biosystems (Foster City, CA) in the campus Biophysics Instrumentation Facility. Cuvette-scale fluorescence measurements were made using a QuantaMasterl photon-counting fluorometer equipped with sample stirring from Photon Technology International (South Brunswick, NJ). [*Methyl*-^{3}H]thymidine incorporation into genomic DNA was quantitated by scintillation counting using a Microbeta TriLux liquid scintillation and luminescence counter from PerkinElmer (Wellesley, MA).

Production of Proteins

Previously, a cysteine residue was installed in place of Gly89 of RNase 1 [23]. The unique sulfhydryl group of this G89C variant was used to construct conjugates with transferrin that had desirable attributes *in vitro*. Accordingly, G89C RNase 1 was employed for the attachment of PEG chains herein.

DNA encoding G89C RNase 1 was created by oligonucleotide-mediated site-directed mutagenesis using a pET22b(+) plasmid that contained cDNA encoding wild-type RNase 1 [11]. The G89C variant of RNase 1 was produced in *E. coli*, the side chain of residue 89 was protected as a mixed disulfide with 2-nitro-5-thiobenzoic acid (NTB), and the NTB-protected G89C RNase 1 was purified as described previously [11]. Wild-type RNase 1, RNase A, and onconase (ONC; which is a cytotoxic homolog of RNase 1 from the Northern leopard frog, *Rana pipiens* [24]) were produced in *E. coli* and purified as described previously [7,25]. The human ribonuclease inhibitor protein (RI) [26] (which is a cytosolic protein with femtomolar affinity for RNase 1 [8]), was produced in *E. coli* and purified as described previously [27,28]. Following purification, each ribonuclease and RI migrated as a single band during sodium dodecyl sulfate–polyacrylamide gel electrophoresis.

Semisynthesis of RNase 1–PEG Conjugates

RNase 1–PEG conjugates were prepared by *S*-alkylation of Cys89 of G89C RNase 1 with a maleimido PEG. The pH of the protein solution containing NTB-protected G89C RNase 1 in cation exchange elution buffer was adjusted from 5 to 7.4–8.0 by the addition of 1.0 M Tris-HCl buffer (pH 7.8–8.0) to 20% (vol/vol). The protecting group was removed by adding DTT (5 equiv) and allowing the reaction to proceed for 2 to 5 minutes, resulting in the immediate generation of the yellow TNB anion [29]. The ribonucleases were separated from DTT, TNB, and salt by using a HiTrap desalting column equilibrated with PBS. A 10-fold molar excess of maleimido PEGs **1**, **2**, or **3** (Figure 1*A*) was dissolved in an equivalent volume of PBS (relative to the volume of ribonuclease-containing solution) and added to the solution containing the deprotected ribonuclease (final [ribonuclease]: ~200 μM). Alkylation reactions were allowed to proceed at room temperature for ~2 hours or overnight at 4°C. Any remaining maleimide groups were quenched by the addition of DTT to a final concentration of 2 mM. To lessen the concentration of residual salt, reactions were diluted to 50 ml with 50 mM sodium acetate buffer (pH 5.0) and dialyzed overnight against 4 l of 50 mM sodium acetate buffer (pH 5.0).
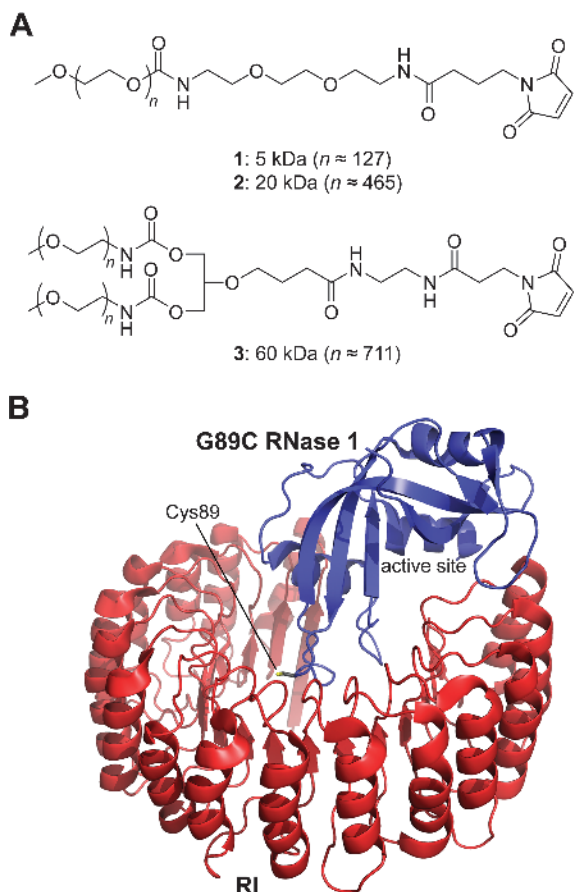
Figure 1. Structures of relevant molecules. (A) Maleimido PEGs used for the preparation of RNase 1–PEG conjugates. (B) A model of the complex between G89C RNase 1 and RI. The model was built by replacing Gly89 in Protein Data Bank (PDB) entry 1z7x [8] with a cysteine residue. The enzymatic active site and side chain of Cys89 are indicated explicitly.

The purification of RNase 1–PEG conjugates relied on the differential affinity for a cation exchange resin. The dialyzed reaction mixtures were applied to a column of HiTrap SPHP cation exchange resin equilibrated with the same buffer and eluted from the resin with a linear gradient of NaCl (0–0.65 M) in 50 mM sodium acetate buffer (pH 5.0). Purification of the highly shielded 60-kDa mPEG$_2$–G89C RNase 1 required dilution of the dialyzed reaction mixture to reduce the salt concentration. RNase 1–PEG conjugates were purified further by chromatography using HiLoad 26/60 G200 Superdex gel filtration resin equilibrated with 50 mM sodium acetate buffer (pH 5.0) containing NaCl (0.10 M) and NaN$_3$ (0.05% wt/vol).

Analyses of RNase 1–PEG Conjugates In Vitro

Analytical size exclusion chromatography.   The hydrodynamic volume of the RNase 1–PEG conjugates was estimated with size exclusion chromatography. A 1.0 mg/ml solution of a conjugate in gel filtration buffer was applied to a HiLoad 26/60 Superdex G200 gel filtration column and eluted with 50 mM sodium acetate buffer (pH 5.0) containing NaCl (0.10 M) and NaN$_3$ (0.05% wt/vol) at a flow rate of 4 ml/min. Gel filtration standards were prepared and separated using the same column according to the guidelines of the manufacturer.

Assays of catalytic activity.   The ribonucleolytic activity of RNase 1–PEG conjugates was determined by assaying their ability to cleave the hypersensitive fluorogenic substrate 6-FAM-dArUdAdA-6-TAMRA [30]. The MES used to prepare the assay buffer was purified by anion exchange chromatography to remove trace amounts of oligomeric vinylsulfonic acid, which is a by-product of commercial buffer synthesis and a potent inhibitor of ribonucleolytic activity [31].

Assays of binding to the RI.   The ability of human RI to bind to RNase 1–PEG conjugates was determined by using a fluorescence-based competition assay [28,32].

Assays of cytotoxicity.   RNase 1–PEG conjugates were tested for their ability to inhibit the in vitro proliferation of K-562 cells, which are especially vulnerable to ribonuclease cytotoxins [33]. The assays monitor the incorporation of [*methyl-*^{3}H]thymidine into the cellular DNA, which is lessened on apoptosis elicited by ribonucleases [34]. Onconase served as a positive control. All cytotoxicity assays were performed at least three times. Half-maximal inhibitory concentration (IC$_{50}$) values were calculated by fitting the data to a sigmoidal dose-response curve using nonlinear regression analysis [28].

Xenograft Studies

PEG conjugates of RNase 1 were tested for their ability to suppress the growth of human tumors implanted into the flanks of athymic mice. The A549 lung tumor cell line was selected for its ability to proliferate in mice, low rate of spontaneous regression, and clinical relevancy. Moreover, A549 cells had been shown previously to be more refractory than other lines to ribonucleases in vitro [28]. These cells were grown in Dulbecco's modified Eagle's medium containing FBS (10% vol/vol). Xenograft models were created by implanting 3.27×10^6 cells into the right rear flank of 43 five- to six-week-old male athymic (*nu/nu*) mice. These animals were used in the treatment group (five mice/conjugate × three conjugates/dose × two doses), positive control (erlotinib; seven mice), and negative control (vehicle = PBS;

six mice). Tumors were allowed to grow to an average size of ~75 mm^3 before initiation of treatment. All treatments were administered by intraperitoneal injection of a volume based on the body weight of the animal (10 μl/g). The mass of the PEG conjugate that was used to calculate the administered dose included the mass of both the ribonuclease and the pendant PEG. Tumor size was measured twice weekly using calipers, and percent tumor growth inhibition (%TGI) was calculated as described previously [11]. Mice were weighed to reveal severe off-target effects.

Pharmacokinetic Studies

Ribonucleolytic activity remaining in the serum of CD-1 mice was used to assess the pharmacokinetic profile of PEGylated ribonucleases. The method was similar to one reported previously [35], except for the assay used to quantify ribonucleolytic activity [22].

Results and Discussion

A pendant PEG moiety can confer clinical benefit to several small human proteins, including human growth hormone (Somavert), erythropoietin (Micera), and interferons α2a (Pegasys) and α2b (Pegintron) [15]. All extant PEGylated drugs, however, act on extracellular targets. Manifesting the cytotoxic activity of RNase 1 requires its entry into the cytosol. Thus, for our intent, a pendant PEG moiety could be a "double-edged sword" [36]. The increased hydrodynamic volume imposed by the PEG could enhance persistence in circulation but also hinder the traversal of a lipid bilayer, which is necessary for entry into the cytosol. To probe this dichotomy, we elaborated the G89C variant of RNase 1 with pendant PEGs of different size (Figure 1) and assessed the attributes of the ensuing conjugates both in vitro and in vivo.

Attributes of RNase 1–PEG Conjugates In Vitro

A pendant PEG increased the viscosity radius of a ribonuclease (Figure 2). As expected, the viscosity radius correlated with the molecular mass of the PEG moiety: 5 kDa < 20 kDa < 60 kDa.

A small or large PEG moiety at residue 89 had a negligible effect on the ability of RNase 1 to catalyze the cleavage of 6-FAM-dArUdAdA-6-TAMRA
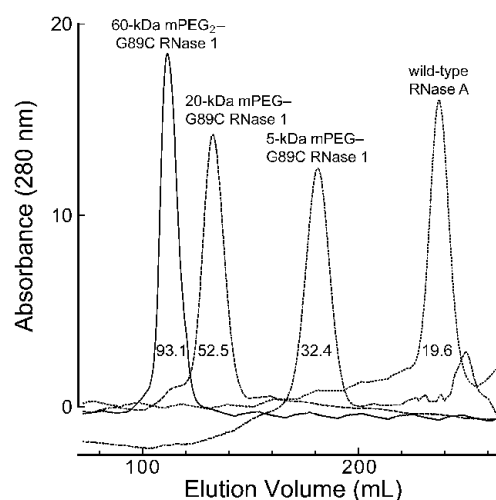
Figure 2. Size exclusion chromatographic profile of RNase 1–PEG conjugates. The values within each peak refer to the calculated viscosity radius [40].

Table 1. Attributes of RNase 1–PEG Conjugates *In Vitro.*

Ribonuclease	k_{cat}/K_M (10^7 M^{-1} s^{-1})*	K_d (nM)[†]	IC$_{50}$ (µM)[‡]
Wild-type RNase 1	2.9 ± 0.1	2.9×10^{-7}	>25
5-kDa mPEG–G89C RNase 1	2.6 ± 0.3	<1.4	>50
20-kDa mPEG–G89C RNase 1	6.8 ± 0.1	<1.4	>50
60-kDa mPEG$_2$–G89C RNase 1	6.1 ± 0.3	<1.4	>50
ONC	0.0018 ± 0.00005	150 ± 50	0.22 ± 0.01

*Values of k_{cat}/K_M (±SE) are for the catalysis of 6-FAM-dArU(dA)$_2$-6-TAMRA cleavage at room temperature in 0.10 M MES-NaOH buffer (pH 6.0) containing NaCl (0.10 M). The values for RNase 1 and ONC were reported previously [11].

[†]Values of K_d (±SE) are for the complex with human RI at room temperature. The values for wild-type RNase 1 [8] and ONC [37] were reported previously.

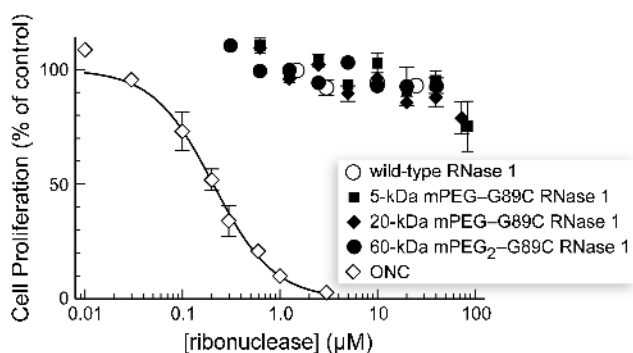[‡]Values of IC$_{50}$ (±SE) are for the incorporation of [*methyl*-^{3}H]thymidine into the DNA of K-562 cells. Data are from Figure 3.

(Table 1). Apparently, this distal location does not impede the substrate from gaining access to the active site (Figure 1*B*). Yet, RI retained notable affinity for the RNase 1–PEG conjugates (Table 1). This sensitivity is likely a result of the extremely high affinity of RI for wild-type RNase 1 [8], as well as the orientation of the side chain of residue 89. Although this residue is at the RI–RNase 1 interface [23], its side chain is oriented nearly perpendicular to the major plane of the RI molecule (Figure 1*B*).
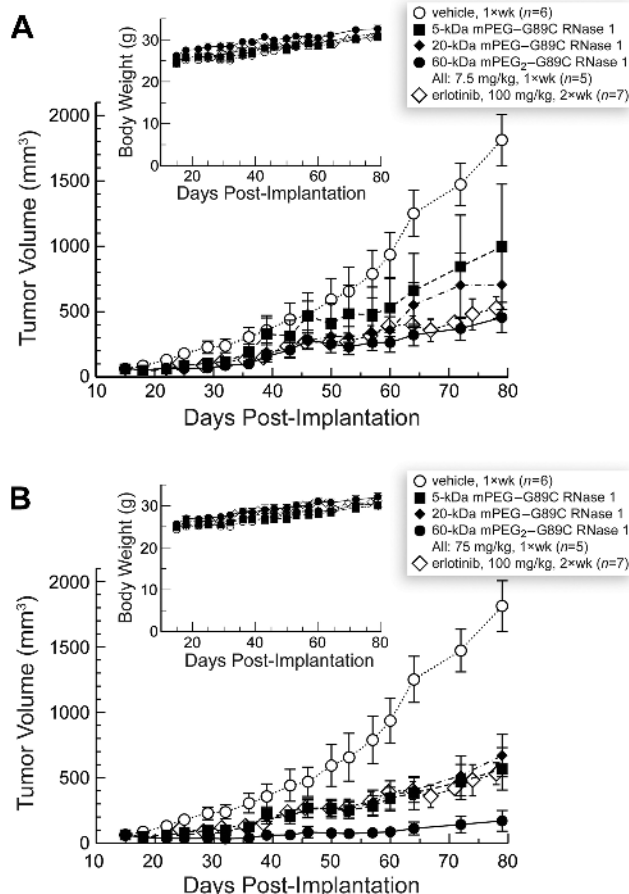
The RNase 1–PEG conjugates had no discernable effect on the proliferation of K-562 cells *in vitro* (Table 1 and Figure 3). Likewise, the RNase 1–PEG conjugates had no effect on the proliferation of A549 cells *in vitro* (data not shown). These data are consistent with a detrimental effect of PEG on membrane translocation, along with the residual affinity for RI, which is known to suppress cytotoxic activity *in vitro* [7,8].

Efficacy of RNase 1–PEG Conjugates in a Xenograft Model

The three RNase 1–PEG conjugates inhibited the growth of solid human tumors in a mouse xenograft model (Figure 4). Tumor growth inhibition by RNase 1–PEG conjugates was more pronounced at a higher dose and for conjugates with larger PEG moieties (Figure 5). More specifically, values of %TGI correlated with those of viscosity radii (cf. Figures 2 and 5). The enhanced efficacy of the larger conjugates is attributable to their longer persistence in circulation, which is known to correlate with PEG molecular mass [38]. Our pharmaco-
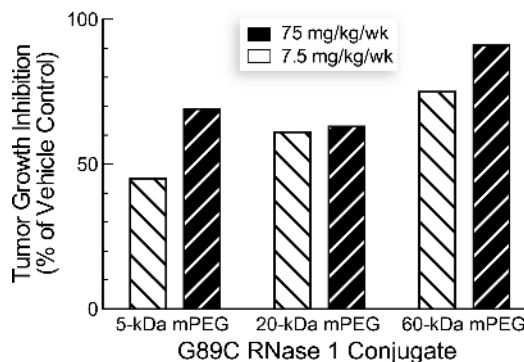
Figure 4. Effect of PEGylated variants of RNase 1 on the tumor volume and body weight (insets) of *nu/nu* mice with xenograft models of human A549 lung tumors. Data are the mean (±SE) for *n* animals. (A) Low dose (7.5 mg/kg per week). (B) High dose (75 mg/kg per week). Data for vehicle- and erlotinib-treated animals are shown in both panels.

kinetic analyses are consistent with this explanation—larger PEG moieties did indeed increase the persistence of a conjugate in serum (Figure 6). The increased persistence is likely due to a decreased rate of glomerular filtration [39,40].

The ability of the larger conjugates to inhibit tumor growth is even greater than suggested by the data depicted in Figure 4. The indicated

Figure 3. Effect of PEGylated variants of RNase 1 on the proliferation of K-562 cells. The incorporation of [*methyl*-^{3}H]thymidine into cellular DNA was used to monitor the proliferation of K-562 cells in the presence of ribonucleases. Data are the mean (±SE) from at least three separate experiments carried out in triplicate.

Figure 5. Effect of PEGylated variants of RNase 1 on tumor growth inhibition (%TGI) of *nu/nu* mice with xenograft models of human A549 lung tumors. Values are from day 79 (Figure 4).
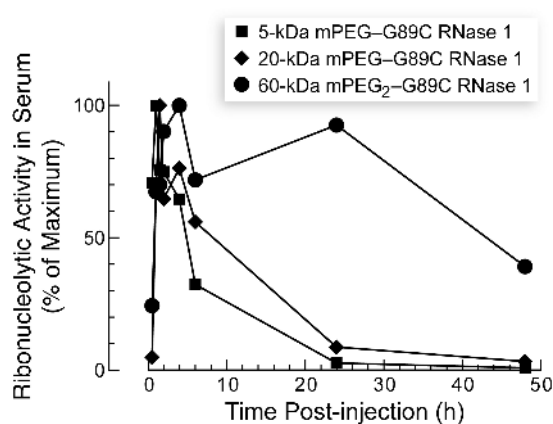
Figure 6. Effect of PEGylation of RNase 1 on its persistence in the circulation of *nu/nu* mice. Blood was drawn at known times after ribonuclease administration.

dose (7.5 or 75 mg/kg) includes the mass of the polymer. Because the molecular mass of RNase 1 is 14.6 kDa, a weekly 7.5 mg/kg dose of the 5-, 20-, or 60-kDa PEG conjugate corresponds to only 383, 217, or 101 nmol/kg, respectively. Thus, mice at a particular dosing level received nearly four-fold as many molecules of the 5-kDa PEG conjugate than the 60-kDa PEG conjugate.

Considering the dosage in molecular rather than mass terms also highlights an advantage of using an enzymatic catalyst as a drug, a few molecules can have a large effect. A weekly dose of 7.5 mg/kg of the 60-kDa PEG conjugate inhibited the growth of tumors at a level indistinguishable from that of a biweekly dose of 100 mg/kg erlotinib (Figure 4*A*). This tyrosine kinase inhibitor was approved in 2004 for the treatment of non–small cell lung cancer [41]. Because erlotinib hydrochloride has a molecular mass of 429.90 Da, treated mice received 0.47 mmol/kg each week. Hence, we estimate that 60-kDa mPEG$_2$–G89C RNase 1 is approximately $(0.47\ \text{mmol/kg})/(101\ \text{nmol/kg}) = 5 \times 10^3$-fold more efficacious than erlotinib. We are not aware of any other human protein that can be endowed with such a high level of preclinical utility by modifying a single amino acid residue.

None of the RNase 1–PEG conjugates exhibited systemic toxicity to the animals as evidenced by their maintenance of body weight throughout the duration of the studies (Figure 5, *insets*). These data indicate that the toxicity of the RNase 1–PEG conjugates toward neoplastic cells is selective *in vivo*.

Basis for the Therapeutic Index of RNase 1–PEG Conjugates

RNase 1 conjugated to human antibody fragments that are directed against tumor-associated antigens has shown promise in preclinical studies [42–44]. In those conjugates, specificity derives largely from the antibody fragment, which is also likely to enhance pharmacokinetics. What is the basis for the favorable therapeutic index demonstrated by the RNase 1–PEG conjugates (Figure 5)?

To date, two contributing factors have been implicated for the cancer cell selectivity of RNase 1 and its homologs *in vitro*. First, cancer cells are more anionic than comparable noncancerous cells [45–47]. Accordingly, Coulomb's law increases preferentially their uptake of highly cationic molecules, such as RNase 1–PEG conjugates [9,48]. Second, cancer cells have an enhanced rate of endocytosis [49] and could take up RNase 1–PEG conjugates more rapidly than do noncancerous cells.

An additional factor is likely to contribute to the favorable therapeutic index of the RNase 1–PEG conjugates *in vivo*. The enhanced permeability and retention effect is a universal characteristic of solid tumors [50,51]. Some of the unique aspects of tumor physiology that contribute to the enhanced permeability and retention effect are the increased permeability of tumor vasculature as well as the poor lymphatic drainage of tumor tissues. The ensuing diminished plasma clearance of macromolecules could combine with architectural differences between normal and neoplastic tissues to accumulate RNase 1–PEG conjugates near tumors. In addition, the large size of the conjugates could extend their retention in tumor tissue, as in circulation (Figure 6).

Conclusions

The site-specific conjugation of a PEG moiety is a promising strategy for the development of cancer chemotherapeutic agents based on RNase 1. Attaching a PEG moiety to residue 89 of RNase 1 preserves catalytic activity, and the ensuing RNase 1–PEG conjugates exhibit marked activity for inhibiting the growth of tumors in xenograft mouse models without detectable systemic toxicity. The antitumoral activity of these conjugates *in vivo* as well as their persistence in circulation increases with PEG size, consistent with the passive accumulation in solid tumors as a key to efficacy. This work provides validation for PEGylated human pancreatic ribonucleases as cancer chemotherapeutic agents.

References

[1] Benito A, Ribó M, and Vilanova M (2005). On the track of antitumour ribonucleases. *Mol Biosyst* **1**, 294–302.

[2] Arnold U (2008). Aspects of the cytotoxic action of ribonucleases. *Curr Pharm Biotechnol* **9**, 1615–1622.

[3] Sorrentino S (2010). The eight human "canonical" ribonucleases: molecular diversity, catalytic properties, and special biological actions of the enzyme proteins. *FEBS Lett* **584**, 2194–2200.

[4] Raines RT (1998). Ribonuclease A. *Chem Rev* **98**, 1045–1065.

[5] Marshall GR, Feng JA, and Kuster DJ (2008). Back to the future: ribonuclease A. *Biopolymers* **90**, 259–277.

[6] Cuchillo CM, Nogués MV, and Raines RT (2011). Bovine pancreatic ribonuclease: fifty years of the first enzymatic reaction mechanism. *Biochemistry* **50**, 7835–7841.

[7] Leland PA, Staniszewski KE, Kim B-M, and Raines RT (2001). Endowing human pancreatic ribonuclease with toxicity for cancer cells. *J Biol Chem* **276**, 43095–43102.

[8] Johnson RJ, McCoy JG, Bingman CA, Phillips GN Jr, and Raines RT (2007). Inhibition of human pancreatic ribonuclease by the human ribonuclease inhibitor protein. *J Mol Biol* **368**, 434–449.

[9] Johnson RJ, Chao T-Y, Lavis LD, and Raines RT (2007). Cytotoxic ribonucleases: the dichotomy of Coulombic forces. *Biochemistry* **46**, 10308–10316.

[10] Rutkoski TJ and Raines RT (2008). Evasion of ribonuclease inhibitor as a determinant of ribonuclease cytotoxicity. *Curr Pharm Biotechnol* **9**, 185–199.

[11] Rutkoski TJ, Kink JA, Strong LE, Schilling CI, and Raines RT (2010). Antitumor activity of ribonuclease multimers created by site-specific covalent tethering. *Bioconjug Chem* **21**, 1691–1702.

[12] Quintessence Biosciences, Inc (2009). A study of QBI-139 in subjects with advanced solid tumors. In *ClinicalTrials.gov* [Internet]. National Library of Medicine, Bethesda, MD. Cited 27 March 2013. Available from http://clinicaltrials.gov/show/NCT00004451 (NLM identifier: NCT00818831).

[13] Greenwald RB, Conover CD, and Choe YH (2000). Poly(ethylene glycol) conjugated drugs and prodrugs: a comprehensive review. *Crit Rev Ther Drug Carrier Syst* **17**, 101–161.

[14] Harris JM and Chess RB (2003). Effect of pegylation on pharmaceuticals. *Nat Rev Drug Discov* **2**, 214–221.

[15] Kling J (2013). PEGylation of biologics. *Bioprocess Int* **11**(3), 34–43.

[16] Souček J, Škvor J, Poučková P, Matoušek J, Slavík T, and Matoušek J (2006). Mung bean sprout (*Phaseolus aureus*) nuclease and its biological and antitumor effects. *Neoplasma* **53**, 402–409.

[17] Matoušek J, Podzimek T, Pouèková P, Stehlík J, Škvor J, Souček J, and Matoušek J (2009). Antitumor effects and cytotoxicity of recombinant plant nucleases. *Oncol Res* **18**, 163–171.

[18] Matoušek J, Podzimek T, Pouèková P, Stehlik J, Škvor J, Lipovova P, and Matoušek J (2010). Antitumor activity of apoptotic nuclease TBN1 from *L. esculentum*. *Neoplasma* **57**, 339–348.

[19] Michaelis M, Cinatl J, Cinatl J, Pouèková P, Langer K, Kreuter J, and Matousek J (2002). Coupling of the antitumoral enzyme bovine seminal ribonuclease to polyethylene glycol chains increases its systemic efficacy in mice. *Anticancer Drugs* **13**, 149–154.

[20] Matoušek J, Pouèková P, Hloušková D, Zadinová M, Souček J, and Škvor J (2004). Effect of hyaluronidase and PEG chain conjugation on the biologic and antitumor activity of RNase A. *J Control Release* **94**, 401–410.

[21] Pouèkova P, Škvor J, Gotte G, Vottariello F, Slavík JT, Matoušek J, Laurents DV, Libonati M, and Souček J (2006). Some biological actions of PEG-conjugated RNase A oligomers. *Neoplasma* **53**, 79–85.

[22] Rutkoski TJ, Kink JA, Strong LE, and Raines RT (2011). Site-specific PEGylation endows a mammalian ribonuclease with antitumor activity. *Cancer Biol Ther* **12**, 208–214.

[23] Suzuki M, Saxena SK, Boix E, Prill RJ, Vasandani VM, Ladner JE, Sung C, and Youle RJ (1999). Engineering receptor-mediated cytotoxicity into human ribonucleases by steric blockade of inhibitor interaction. *Nat Biotechnol* **17**, 265–270.

[24] Lee JE and Raines RT (2008). Ribonucleases as novel chemotherapeutics: the ranpirnase example. *BioDrugs* **22**, 53–58.

[25] delCardayré SB, Ribó M, Yokel EM, Quirk DJ, Rutter WJ, and Raines RT (1995). Engineering ribonuclease A: production, purification and characterization of wild-type enzyme and mutants at Gln11. *Protein Eng* **8**, 261–273.

[26] Dickson KA, Haigis MC, and Raines RT (2005). Ribonuclease inhibitor: structure and function. *Prog Nucleic Acid Res Mol Biol* **80**, 349–374.

[27] Klink TA, Vicentini AM, Hofsteenge J, and Raines RT (2001). High-level soluble production and characterization of porcine ribonuclease inhibitor. *Protein Expr Purif* **22**, 174–179.

[28] Rutkoski TJ, Kurten EL, Mitchell JC, and Raines RT (2005). Disruption of shape-complementarity markers to create cytotoxic variants of ribonuclease A. *J Mol Biol* **354**, 41–54.

[29] Ellman GL (1959). Tissue sulfhydryl groups. *Arch Biochem Biophys* **82**, 70–77.

[30] Kelemen BR, Klink TA, Behlke MA, Eubanks SR, Leland PA, and Raines RT (1999). Hypersensitive substrate for ribonucleases. *Nucleic Acids Res* **27**, 3696–3701.

[31] Smith BD, Soellner MB, and Raines RT (2003). Potent inhibition of ribonuclease A by oligo(vinylsulfonic acid). *J Biol Chem* **278**, 20934–20938.

[32] Abel RL, Haigis MC, Park C, and Raines RT (2002). Fluorescence assay for the binding of ribonuclease A to the ribonuclease inhibitor protein. *Anal Biochem* **306**, 100–107.

[33] Leland PA, Schultz LW, Kim B-M, and Raines RT (1998). Ribonuclease A variants with potent cytotoxic activity. *Proc Natl Acad Sci USA* **95**, 10407–10412.

[34] Haigis MC, Kurten EL, and Raines RT (2003). Ribonuclease inhibitor as an intracellular sentry. *Nucleic Acids Res* **31**, 1024–1032.

[35] Tarnowski GS, Kassel RL, Mountain IM, Blackburn P, Wilson G, and Wang D (1976). Comparison of antitumor activities of pancreatic ribonuclease and its cross-linked dimer. *Cancer Res* **36**, 4074–4078.

[36] Fishburn CS (2008). The pharmacology of PEGylation: balancing PD with PK to generate novel therapeutics. *J Pharm Sci* **97**, 4167–4183.

[37] Turcotte RF and Raines RT (2008). Interaction of onconase with the human ribonuclease inhibitor protein. *Biochem Biophys Res Commun* **377**, 512–514.

[38] Yamaoka T, Tabata Y, and Ikada Y (1994). Distribution and tissue uptake of poly(ethylene glycol) with different molecular weights after intravenous administration to mice. *J Pharm Sci* **83**, 601–606.

[39] Maack T (2000). Renal filtration, transport, and metabolism of proteins. In *The Kidney: Physiology and Pathophysiology* (3rd ed). DW Seldin and GH Giebisch (Eds). Lippincott Williams & Wilkins, Philadelphia, PA. pp. 2235–2267.

[40] Fee CJ and Van Alstine JM (2004). Prediction of the viscosity radius and the size exclusion chromatography behavior of PEGylated proteins. *Bioconjug Chem* **15**, 1304–1313.

[41] Cohen MH, Johnson JR, Chen YF, Sridhara R, and Pazdur R (2005). FDA drug approval summary: erlotinib (Tarceva) tablets. *Oncologist* **10**, 461–466.

[42] De Lorenzo C and D'Alessio G (2009). Human anti-ErbB2 immunoagents—immunoRNases and compact antibodies. *FEBS J* **276**, 1527–1535.

[43] Rybak SM, Arndt MA, Schirrmann T, Dübel S, and Krauss J (2009). Ribonucleases and immunoRNases as anticancer drugs. *Curr Pharm Des* **15**, 2665–2675.

[44] Weidle UH, Georges G, and Brinkmann U (2012). Fully human targeted cytotoxic fusion proteins: new anticancer agents on the horizon. *Cancer Genomics Proteomics* **9**, 119–133.

[45] Slivinsky GG, Hymer WC, Bauer J, and Morrison DR (1997). Cellular electrophoretic mobility data: a first approach to a database. *Electrophoresis* **18**, 1109–1119.

[46] Ran S, Downes A, and Thorpe PE (2002). Increased exposure of anionic phospholipids on the surface of tumor blood vessels. *Cancer Res* **62**, 6132–6140.

[47] Dube DH and Bertozzi CR (2005). Glycans in cancer and inflammation—potential for therapeutics and diagnostics. *Nat Rev Drug Discov* **4**, 477–488.

[48] Chao T-Y, Lavis LD, and Raines RT (2010). Cellular uptake of ribonuclease A relies on anionic glycans. *Biochemistry* **49**, 10666–10673.

[49] Levine MN, Hoang TT, and Raines RT (2013). Fluorogenic label to quantify the cytosolic delivery of macromolecules. *Chem Biol* **20**, 614–618.

[50] Maeda H, Wu J, Sawa T, Matsumura Y, and Hori K (2000). Tumor vascular permeability and the EPR effect in macromolecular therapeutics: a review. *J Control Release* **65**, 271–284.

[51] Fox ME, Szoka FC, and Frechet JMJ (2009). Soluble polymer carriers for the treatment of cancer: the importance of molecular architecture. *Acc Chem Res* **42**, 1141–1151.